

Molecular Dynamics Simulations of Polytetrafluoroethylene at Glassy Transition Temperature

R. Al-Nsour^{*}, J. Hackett^{*}, B. Hinderliter,^{**} and M. Gad-el-Hak^{*}

^{*}Virginia Commonwealth University, Richmond, VA, USA, alnsourra@vcu.edu

^{**}University of Minnesota, Duluth, MN, USA

ABSTRACT

The current research utilizes Molecular Dynamics Simulations to model and predict the PTFE glassy transition temperature using OPLS-AA PTFE force-field parameters. Achieving the aforementioned objective involved performing two major tasks. First, building PTFE amorphous structure using Material Studio®. Second, performing Molecular Dynamics simulations using NAMD®. The latter task involves a polymer relaxation process, which was started with NVT followed by NPT ensemble simulations to predict PTFE glassy transition temperature. The results of our simulations were in good agreement with experimental findings.

Keywords: polytetrafluoroethylene, glassy transition temperature, molecular dynamics simulations, amorphous structure.

1 INTRODUCTION

Fluoropolymers are employed in countless end-user applications across several industries [1-4]. One such Fluoropolymer is Polytetrafluoroethylene (PTFE). This research is concerned with studying and understanding the thermal and mechanical behavior of PTFE around its glass transition temperature. Such understanding is critical to predict PTFE behavior in diverse service environments and for allowing bottom up design of improved polymers for specific applications. The glassy transition temperature is defined as “the temperature at which the forces holding the distinct components of an amorphous solid together are overcome by thermally induced motions within the time scale of the experiment, so that these components are able to undergo large-scale molecular motions on this time scale, limited mainly by the inherent resistance of each component to such flow” [5]. The chain backbone degree of rotation plays a vital role in deciding the glassy transition temperature where the macromolecule backbone movements are governed by the molecular weight and the non-bonded interaction forces. To this end, as the molecular weight and the intermolecular forces increase, the degree of molecular movements becomes more limited which results in higher glassy transition temperature. The occurrence of the glassy transition temperature causes many changes in

polymers properties such as their stiffness, thermal conductivity, and specific volume. Research evidence indicates that the behavior of thermoplastics above the glassy transition temperature is elastic. This is due to the intermolecular forces being overcome by the thermally induced molecular motions for polymer segments. More specifically, as temperature increases, thermoplastics gradually soften and lose their rigidity (i.e. hardness) until they eventually melt. Several experimental studies have computed the glassy transition temperature of PTFE polymer and Tetrafluoroethylene (TFE) monomer with values ranging between 160-400K [6-11].

While a plethora of experiments have investigated the mechanical properties of PTFE [12], examining these properties using molecular dynamics simulations (MD) remains in its infancy [11]. In particular, the current body of MD research on PTFE has primarily focused on studying PTFE phases, its physical nature, and its helical conformational structure [13-15]. The present study is one of the first MD simulations to research PTFE behavior around the glassy transition temperature.

2 METHODOLOGY

2.1 OPLS-AA Force-Field Potential

MD simulates the interactions and motions of molecules based on forces between atoms. These interactions were represented in molecular mechanics models (i.e., force fields) such as OPLS [16] AMBER [17], and CHARMM [18]. The current work utilizes OPLS-AA force-field model; developed by Jorgensen and Tirado-Rives [16], which continues to be one of the most accurate molecular mechanics models. The energy potential function encompasses all the terms that represent interactions at the atomic level, which will be used to obtain complete and comprehensive MD simulations. In addition, this model offers parameter transferability from smaller to bigger oligomers [19]. The OPLS model is presented as

$$E_{Total} = \sum_{bonds} kr(r-r_{eq})^2 + \sum_{angles} K\theta(\theta-\theta_{eq})^2 + \sum_{n=1}^n V_n(1 + \cos(n\phi - f_n) + \left(\sum_{vdw} 4\varepsilon_{ij} \left[\left(\frac{\sigma_{ij}}{r_{ij}} \right)^{12} - \left(\frac{\sigma_{ij}}{r_{ij}} \right)^6 \right] + \sum_{electrostatic} \frac{q_i q_j}{4\varepsilon_0 r_{ij}} \right) \quad (1)$$

where k_r refers to the bond constant, k_θ refers to the angle constant, r_{eq} refers to the equilibrium bond value, θ_{eq} refers to the equilibrium angle value, ϕ refers to the dihedral angle, V_n refers to the dihedral coefficient, f_n refers to the phase angle, ε_{ij} refers to the potential well depth, σ_{ij} and refers to the distance where Lennard-Jones potential is zero or the minimum, r_{ij} refers to the distance between a pair of atoms, q_i and q_j refer to the electrostatic charges for pair of atoms, and ε_0 refers to the dielectric constant of vacuum. The OPLS-AA force fields parameters that we used in this research are presented in Table 1.

Interaction	Parameters			
bond	k_r (kcal/mol/Å ²)		r_{eq} (Å°)	
C-F	367.0		1.332	
C-C	268.0		1.529	
Angle	k_θ (kcal/mol/rad ²)		θ_{eq} (deg)	
C-F-C	77.00		109.10	
C-C-F	50.0		109.50	
C-C-C	58.35		112.70	
Dihedrals	V_n (kcal/mol)			
	V_1	V_2	V_3	V_4
F-C-C-F	-2.500	0.000	0.250	0.000
C-C-C-F	0.300	0.000	0.400	0.000
C-C-C-C	6.622	0.948	-1.388	-2.118
Electrostatic	Charges(e)			
F	-0.12			
CF2	-0.24			
CF3	-0.36			
Lennard Jones (VDW)	σ (Å°)		ε_{ij} (kcalmol ⁻¹)	
F	2.95		0.053	
C	3.50		0.066	

Table 1: PTFE force-field paramter adopted from [20]

The CF2 refers to the carbon atom that is connected to two flourine atoms, and CF3 refers to the carbon atom that is connected to three flourine atoms.

2.2 Amorphous Structure

The amorphous structure refers to the disarrangements of the molecules where the carbon chains are disordered due to the absence of crystallinity. In MD simulations studies, examining the glassy transition temperature is contingent on obtaining the amorphous configuration. Research evidence reveals that polymer properties such as the specific volume will differ as the polymer passes the glassy transition when it is in the amorphous phase structure, however, no variation in the specific volume will occur when the polymer passes the glassy transition while it is in the crystalline structure [21]. This is because the polymer melt and the polymer glass for an amorphous structure are related to the same thermodynamic state at the glassy transition. As noted by Turnbull and Cohen [21], at this state “the free energy of the amorphous phase should be a minimum when this free volume is distributed at random. Such a random distribution of free volume can occur in the amorphous but not in the crystalline phase”.

MD simulations literature offers three ways to obtain the amorphous structure as follows: Material Studio amorphous builder. This tool has been used by several researchers for PTFE simulation related work [e.g., 14, 22, 23].

The gradual compression of the simulation cell box (i.e. increasing the pressure) until it reaches the gaseous phase. [24, 25].

The simulated annealing (SA) criteria. This method has been used by many researchers in condensed phase simulations. For example, Dai et al. [26] obtain the amorphous configuration for polypropylene using SA in NAMD. The annealing process is initiated by the gradual heating of the crystalline polymer to a high temperature where all atoms are randomly softened to the melt phase. This step is followed by a slow cooling process to relax the polymer configuration from the internal stresses after being heated to high temperatures. In MD simulations, the heating and cooling cycle is consistently repeated over time in order for the molecular segments to overcome the high energy barriers in the crystalline polymer and until the amorphous structure is obtained [27].

3 DISCUSSION AND RESULTS

As pointed out earlier, modeling the PTFE glassy transition temperature involved performing two major tasks. We began by building PTFE amorphous structure. To this end, we used a PTFE chain consisting of 64 Carbon and 130 Fluorine atoms. Next, we utilized Material Studio [28] amorphous module to obtain the amorphous structure. Figure 1 displays the resulting amorphous structure with 10 chains where the total number of atoms equal to 1940. The amorphous builder is based on Monte Carlo algorithm which reduces the atoms VDW radii by at least 70% to prevent the VDW repulsive interactions between atoms. In

addition, it should be noted that when using the Monte Carlo algorithm ensures that the dihedral angles will not overlap but rather follow the Boltzmann distribution.

With the amorphous structure successfully built, the next task was to compute the glass transition temperature by performing a relaxation simulations. The relaxation procedure started with NVT MD simulations at high temperature (550K), where the macroscopic boundary conditions were kept constant. This step was followed by NPT MD simulations at high temperature (550K). As the system moved from one equilibrated state to another, it was minimized and equilibrated using NPT. Finally we performed NPT annealing to the desired temperature for enough time to reach the thermodynamic equilibrium. Three target temperatures were used in the annealing process as follows: a temperature lower than the glassy transition temperature (i.e, 150K), a temperature around the glassy transition temperature (i.e, 350K), and a temperature higher than the glassy transition temperature (i.e, 450K). The cooling process was performed slowly and gradually to allow any needed transformations to occur. Otherwise, the system would be quenched, deformed and tricked to unfavorable minimum local energy. For example, The relaxation to a temperature lower than PTFE glassy transition temperature takes 50000 fs with cooling rate of 1.0K/ps as shown in Figure 2. It should be noted that high cooling rates were used for the high temperature targets and low cooling rates for low temperature targets, for example for the annealing to 450K and 350K we use the high rate while for the annealing to 150K we use the slow cooling rate.

The relaxation simulations were performed with 1 femtosecond (fs) timestep. Nose-Hoover algorithm was used to control pressure [29]. Further, to control intermolecular interactions, a 12 Å cut-off radius and particle mesh Ewald method [30] were used.

The glassy transition temperature for PTFE is represented in Figure 3. The kink in the volume evolution as a function of temperature appears about 398K, which falls in the glassy transition temperature rang between 160K to 400K from the experimental approach findings, for example Sperati and Starkweather [10] found that Tetrafluoroethylene (TFE) glassy transition temperature to be around 160K, Araki [31] found PTFE glassy transition temperature to be around 396K for different PTFE samples. This wide range would be due to the different in molecular weight between the Tetrafluoroethylene and PTFE.

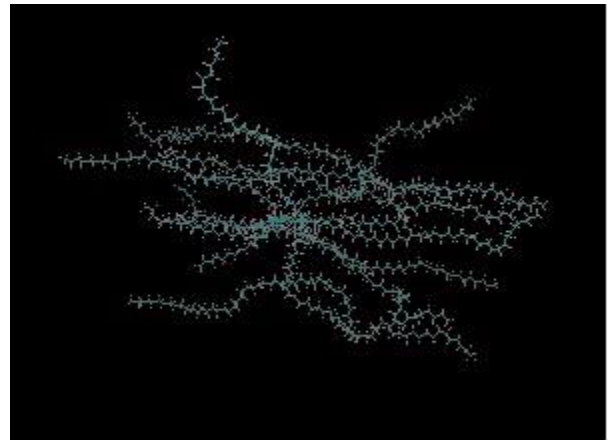


Figure 1: PTFE amorphous structure.

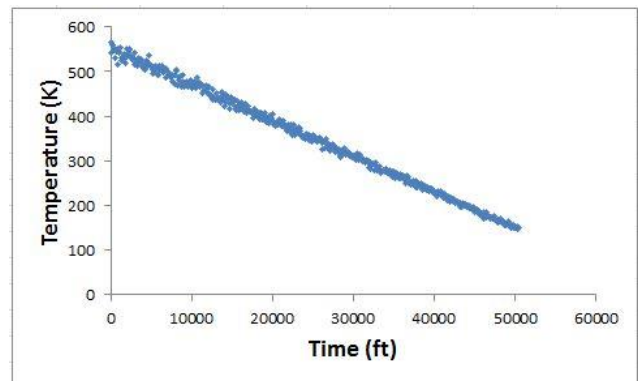


Figure 2: Low rate PTFE relaxation .

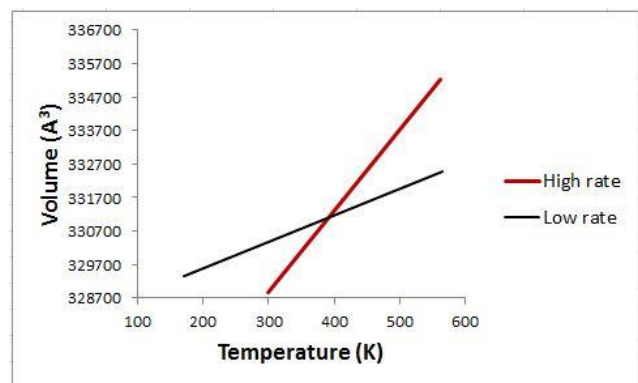


Figure 3: PTFE glassy transition temperature is computed from volume evolution as a function of temperature.

4 CONCLUSIONS

In the present work, we use the molecular dynamics simulations to compute the glassy transition temperature for an amorphous PTFE, the simulations were performed for different temperatures, higher, around and lower than the glassy transition temperature. The glassy transition temperature has been detected from the intersection between the high and low rate of PTFE cooling simulations. The simulations results were in good agreement with the experiments findings. This work in progress will be continued to investigate PTFE glassy transition temperature with different molecular weights.

REFERENCES

- [1] L. Brasile, J. Clarke, in, Google Patents, 1997.
- [2] U. Gross, G. Papke, S. Rüdiger, *Journal of fluorine chemistry*, 61 (1993) 11-16.
- [3] D.A. Long, D. Long, *Raman spectroscopy*, McGraw-Hill New York, 1977.
- [4] S. Ebnesajjad, in, *Applied Plastics Engineering Handbook*, Elsevier Inc, 2011.
- [5] H.F. Mark, *Encyclopedia of Polymer Science and Technology: Reinforced plastics to starch*, Interscience publishers, 1970.
- [6] S.F. Lau, J.P. Wesson, B. Wunderlich, *Macromolecules*, 17 (1984) 1102-1104.
- [7] W.S. Durrell, E.C. Stump Jr, P.D. Schuman, *Journal of Polymer Science Part B: Polymer Letters*, 3 (1965) 831-833.
- [8] J. Sauer, D. Kline, *Journal of Polymer Science*, 18 (1955) 491-495.
- [9] J.W. Nicholson, *The chemistry of polymers*, Royal Society of Chemistry, 2011.
- [10] C. Sperati, H. Starkweather, *Fortschritte Der Hochpolymeren-Forschung*, (1961) 465-495.
- [11] P. Rae, D. Dattelbaum, *Polymer*, 45 (2004) 7615-7625.
- [12] E. Konova, Y.E. Sakhno, S. Khatipov, V. Klimenko, S. Sychkova, T. Sakhno, *PHYSICS AND CHEMISTRY OF SOLID STATE*, 12 (2011) 1013-1017.
- [13] M. Sprik, U. Röthlisberger, M.L. Klein, *The Journal of Physical Chemistry B*, 101 (1997) 2745-2749.
- [14] D. Holt, B. Farmer, *Polymer*, 40 (1999) 4673-4684.
- [15] A. Vishnyakov, A.V. Neimark, *The Journal of Physical Chemistry B*, 104 (2000) 4471-4478.
- [16] W.L. Jorgensen, J. Tirado-Rives, *Journal of the American Chemical Society*, 110 (1988) 1657-1666.
- [17] D.A. Case, T.E. Cheatham, T. Darden, H. Gohlke, R. Luo, K.M. Merz, A. Onufriev, C. Simmerling, B. Wang, R.J. Woods, *Journal of computational chemistry*, 26 (2005) 1668-1688.
- [18] A.D. MacKerell Jr, B. Brooks, C.L. Brooks III, L. Nilsson, B. Roux, Y. Won, M. Karplus, *Encyclopedia of computational chemistry*, (1998).
- [19] O. Borodin, G.D. Smith, D. Bedrov, *The Journal of Physical Chemistry B*, 106 (2002) 9912-9922.
- [20] E.K. Watkins, W.L. Jorgensen, *The Journal of Physical Chemistry A*, 105 (2001) 4118-4125.
- [21] D. Turnbull, M.H. Cohen, *The Journal of Chemical Physics*, 34 (1961) 120.
- [22] D. Holt, B. Farmer, *Polymer*, 40 (1999) 4667-4672.
- [23] S.S. Jang, S.T. Lin, T. Çagin, V. Molinero, W.A. Goddard III, *The Journal of Physical Chemistry B*, 109 (2005) 10154-10167.
- [24] O. Okada, K. Oka, S. Kuwajima, K. Tanabe, *Molecular simulation*, 21 (1999) 325-342.
- [25] S.S. Jang, M. Blanco, W.A. Goddard III, G. Caldwell, R.B. Ross, *Macromolecules*, 36 (2003) 5331-5341.
- [26] Z.W. Dai, J. Ling, X.J. Huang, L.S. Wan, Z.K. Xu, *The Journal of Physical Chemistry C*, 115 (2011) 10702-10708.
- [27] P.J. Van Laarhoven, E.H. Aarts, *Simulated annealing*, Springer, 1987.
- [28] F. Module, Accelrys Inc., San Diego, CA, (2011).
- [29] G.J. Martyna, D.J. Tobias, M.L. Klein, *The Journal of Chemical Physics*, 101 (1994) 4177.
- [30] T. Darden, D. York, L. Pedersen, *The Journal of Chemical Physics*, 98 (1993) 10089.
- [31] Y. Araki, *Journal of Applied Polymer Science* 9 (2), 421-427 (1965).